JOURNAL OF COMPUTATIONAL PHYSICS 85, 86–103 (1989)

A Random Vortex Simulation of Falkner–Skan Boundary Layer Flow

D. M. SUMMERS

Department of Mathematics, Napier Polytechnic, 219 Colinton Road, Edinburgh EH14 1DJ, United Kingdom

Received December 7, 1987; revised November 28, 1988

Chorin (*J. Comput. Phys.* **27**, 428 (1978)) applied a random vortex sheet method to the problem of incompressible boundary-layer flow with a uniform external velocity, $U(x) = U_0$. The application of the method is here extended to the case of an external flow field of the form $U(x) = U_0 x^m$, where m is a real number. The method generates time-dependent solutions to the Prandtl equations and these non-similar solutions, in their temporal mean, are compared to the corresponding similar solutions of the Falkner–Skan equation. A visualisation of the spatial structure of the velocity field in the boundary layer is obtained numerically for various values of m.

1. INTRODUCTION

Chorin [1] introduced a random vortex sheet method which provides a grid-free solution procedure for boundary layer flow. The time evolution of such flow is modelled by the translation of Lagrangian vortex sheet elements in the field they collectively induce. The effects of viscosity are represented by a stochastic model: a random walk displacement is imparted to each element at each time step. The no-slip condition at the boundary is effected by the creation of a vortex sheet there at each time step.

The dynamics of 2-dimensional laminar incompressible flow in a boundary layer can be derived (see Schlichting [2], for example) from the Navier–Stokes equations:

$$\frac{\partial u}{\partial t} + u\frac{\partial u}{\partial x} + v\frac{\partial u}{\partial y} = -\frac{\partial p}{\partial x} + \nu\left(\frac{\partial^2 u}{\partial y^2} + \frac{\partial^2 u}{\partial x^2}\right) \tag{1a}$$

$$\frac{\partial v}{\partial t} + u\frac{\partial v}{\partial x} + v\frac{\partial v}{\partial y} = -\frac{\partial p}{\partial y} + \nu\left(\frac{\partial^2 v}{\partial x^2} + \frac{\partial^2 v}{\partial y^2}\right) \tag{1b}$$

together with the continuity equation:

$$\frac{\partial u}{\partial x} + \frac{\partial v}{\partial y} = 0. \tag{1c}$$

0021-9991/89 $3.00

We consider a solid boundary to coincide with $y=0$, with the fluid occupying the half-space $y \geqslant 0$; x is the coordinate in the stream direction, y the coordinate perpendicular to the boundary. The functions $u(x, y)$ and $v(x, y)$ are respectively the stream component of the flow and the component of the flow normal to the boundary; ν is kinematic viscosity.

The thickness of a boundary layer is proportional to $\nu^{1/2}$, thus for slight viscosity this thickness is very much smaller than the stream dimensions of the boundary. Dimensionally this implies $\partial u/\partial y \gg \partial v/\partial x$ and $\partial u/\partial x \ll \partial u/\partial y$. Equation (1a) can be simplified to

$$\frac{\partial u}{\partial t}+u\frac{\partial u}{\partial x}+v\frac{\partial u}{\partial y}=-\frac{\partial p}{\partial x}+\nu\frac{\partial^2 u}{\partial y^2} \tag{2}$$

which, with the continuity equation (1c), constitute the Prandtl boundary layer equations.

Dimensional considerations also show that $\partial p/\partial y \ll \partial p/\partial x$. By setting $\partial p/\partial y = 0$, Eq. (1a) becomes decoupled from (1b) and a solution to Eq. (2) can be found without reference to Eq. (1b). This procedure amounts to making the assumption that the pressure gradient across the boundary layer is negligible.

The boundary conditions associated with the velocity field (u, v) are those consistent with a boundary that is impermeable and one at which a no-slip condition is satisfied, i.e.,

$$v(x, 0) = u(x, 0) = 0.$$

Away from the boundary an external flow is imposed such that

$$\lim_{y \to \infty} u(x, y) = U(x),$$

where $U(x)$ is a prescribed velocity field. Additionally, the time-dependent equation (2) requires an initial condition at $t=0$. The point $x=0$ corresponds to the "leading edge" of the boundary, and the flow must also be specified at this point.

The character of boundary-layer flow has been explored by determining time-stationary solutions to (2). The stationary solution to (2) for which the external stream is constant, i.e., $U(x) = U_0$, corresponds to the classic problem of uniform main stream flow over a semi-infinite flat plate. Since the pressure field, p, is taken to have the uniform spatial structure of the external flow, then Eqs. (2) and (1c) can be transformed into the Blasius equation

$$f''' + ff'' = 0 \tag{3}$$

with $u(x, y) = U_0 f'(\eta)$, and the similarity variable η is given by

$$\eta = y\left[\frac{U_0}{\nu x}\right]^{1/2}.$$

The numerical solution to (3) is the well-known Blasius velocity profile.

Similarity solutions such as this may be of restricted application. However, since they are solutions to an ordinary differential equation they are relatively easy to determine numerically and they do offer a valuable point of comparison for numerical solutions to non-similar flow problems which are more generally governed by the partial differential equations (2) and (1c).

Chorin [1] compared the velocity profile he derived from a random vortex simulation of flow governed by (2) (with $U(x) = U_0$ and $\nu = 10^{-6}$) to the Blasius solution. The non-similar flow was initiated impulsively at $t = 0$; after a developed velocity profile was established, subsequent time averages of the flow were formed. These averages compare well with the Blasius solution to (3) (see Fig. 2 of Ref. [1]). Puckett [3] has investigated in some detail the convergence associated with this solution of the Blasius case. He relates the rate of convergence to the computational parameters of the random vortex sheet method.

Lewis [4] and Lewis and Porthouse [5] have applied a vortex-in-cell method to evaluating Blasius flow (for a viscosity $\nu = 0.05$) in which they achieve an encouraging simulation of the flow profile. In this application, the vortex-in-cell method consists of a fixed grid over the boundary. Although this reduces computational effort, it also effectively abandons an important advantage of purely Lagrangian vortex methods such as Chorin's, namely, that the re-introduction of a grid will also re-introduce numerical diffusion into the solution. This is an important consideration for media of very slight viscosity such as air ($\nu = 10^{-6}$).

Lewis and Porthouse [4] apply their method also to the problem of boundary layer flow with streamwise pressure gradients and achieve—at least for favourable pressure gradients—some measure of agreement with the corresponding similar solution. In this context it would useful to see how the random vortex sheet method of Chorin can be extended to the problem of accelerated or decelerated boundary layer flow.

2. Falkner–Skan Boundary Layer Flow

A class of similarity solution to (2) can be determined (with $\partial u/\partial t = 0$) if we consider external flows of the particular form

$$U(x) = U_0 x^m, \tag{4}$$

where m is a real number. (The Blasius case is recovered by setting $m = 0$.) If we express the pressure field as

$$\frac{\partial p}{\partial x} = U \frac{\partial U}{\partial x},$$

then the Prandtl equations can be transformed into the ordinary differential equation

$$f''' + ff'' + \frac{2m}{m+1}\{1 - (f')^2\} = 0, \tag{5}$$

where the modified stream function, f, depends only on the similarity variable

$$\eta = y\left[\frac{U_0 x^m (m+1)}{2\nu x}\right]^{1/2}. \tag{6}$$

The field (u, v) is defined through

$$u(x, y) = U(x) f'(\eta) \tag{7}$$

and

$$v(x, y) = -\left[\frac{U(x)\nu}{2x(m+1)}\right]^{1/2} \{(m-1)\eta f'(\eta) + (m+1) f(\eta)\}. \tag{8}$$

The prime denotes differentiation with respect to η. The boundary conditions to be satisfied by (5) are

$$f(0) = f'(0) = 0 \qquad \text{and} \qquad f'(\infty) = 1. \tag{9}$$

The physical problem described by an external flow (4) is, for $m > 0$, that corresponding to a favourable external pressure gradient in the stream direction, and, for $m < 0$, to flow under an adverse pressure gradient. In the parameter range $m \in [0, 1]$, $U(x)$ in (4) describes the inviscid flow over a wedge of opening angle $2m\pi/(m+1)$, the case $m = 1$ corresponding to stagnation flow at a wall, and the case $m = 0$ to flow over a flat plate as discussed previously.

Equation (5) has been the subject of much analytical and numerical study, not least because of the interesting multiple solutions which can exist in certain ranges of the parameter m. In the range $m \in [0, 1]$, the existence [6] and uniqueness [7] of solutions to (5) have been established. But multiple solution branches have been discovered numerically by a number of authors in the ranges $m > 1$ and $m < 0$.

The latter range is interesting because it corresponds to the case of adverse pressure gradient. The value $m = -0.0904$ was determined by Hartree [8] (in what was the first detailed numerical study of the Falkner–Skan problem) to be the parameter at which zero shear stress τ_w is achieved at the boundary. For this value of m we can write

$$\tau_w \equiv \left.\frac{\partial u}{\partial y}\right|_{y=0} = \left[\frac{m+1}{2\nu x}\right]^{1/2} f''(0) = 0 \tag{10}$$

and this corresponds to the case of flow separating completely along the boundary. This suggests that $m < -0.0904$ is a regime of separated flow; the physical assumptions implicit to (2) may, of course, be violated if the flow is separating.

Typically, Eq. (5) is solved by a numerical shooting method [9]; $f''(0)$ is guessed, then integrated to large η in order to determine whether condition (9) is satisfied at infinity. For $m < 0$, Hartree [8] found that acceptable solutions to (5) could be found for an infinite number of values of $f''(0)$, and this effectively

establishes the non-uniqueness of $f(\eta)$ in this parameter range. Various additional mathematical (and physical) criteria can be imposed there, however, to restrict the solution space.

For example, Hartree forced uniqueness in the regime $m \in [-0.0904, 0]$ by insisting that the flow solution (considered here as a function of parameter m) be continuous across $m = 0$. Furthermore, "overshoot" was excluded for physical reasons (which some authors have subsequently disputed [10]); this is to say that the case satisfying the inequality $f'(\eta) > 1$ in $\eta < \infty$ was excluded. In addition, the case of reverse flow, i.e., $f''(0) < 0$, was not considered by Hartree.

As these various restrictions are relaxed, the character of the multiple solutions to (5) emerges. For example, reversed flow solutions in $m \in [-0.0904, 0]$ [11, 12] have been discovered, and multiple oscillatory solutions are found to exist in $m < -1$ [10, 13] and in $m > 1$ [13, 14].

This raises a question of obvious interest: what, if anything, can these multiple solutions imply about physical flow? It is in this connection that the time-dependent solutions to (2) may contribute some understanding to the similar solutions of (5), if the latter are interpreted as a temporal mean of the former.

3. Random Vortex Solution of the Prandtl Equations

The boundary layer equations can be expressed in terms of vorticity ξ by taking the curl of the vector form of Eqs. (1). Making the approximations $\partial u/\partial y \gg \partial v/\partial x$ and $\partial u/\partial x \ll \partial u/\partial y$ in the resulting equation, and defining

$$\xi = -\partial u/\partial y, \tag{11}$$

we obtain

$$\frac{\partial \xi}{\partial t} + u\frac{\partial \xi}{\partial x} + v\frac{\partial \xi}{\partial y} = \nu\frac{\partial^2 \xi}{\partial y^2}. \tag{12}$$

Since this single vorticity transport equation expresses the two equations (1a) and (1b) in the boundary layer approximation, we are no longer required to force any decoupling between momentum equations. This is to say, the pressure field in the boundary layer is no longer constrained to assume that of the external flow, although dimensional considerations still imply $\partial p/\partial y \ll \partial p/\partial x$.

The random vortex sheet solution of (12) is effected by discretising the vorticity distribution ξ into a finite collection of vortex sheet segments (or elements). Detailed description of the theory of the numerical method is provided by a number of authors [1, 15–18]. A computer program—which the present author has modified in order to accommodate the more general external flow field, (4), of this paper—has been published by Cheer [19].

The basic strategy of the method is to represent the flow dynamics in the boundary layer by a Lagrangian description expressed in terms of discrete vortex sheet elements, then to solve (12) to determine the evolving displacement of each element. Equation (12) is solved in two fractional time steps. In the first of these the

segments are transported by the advective contribution in (12); in the second fractional step the diffusion of ξ is represented by a stochastic simulation: the segments are made to undergo a set of random-walk displacements.

Consider a collection of vortex sheet segments, each of length h and of strength $\{\gamma_i\}$ located at points $\{(x_i, y_i)\}$. The parameter γ_i is essentially the velocity jump across the sheet element,

$$\gamma_i = \lim_{\delta y \to 0} \int_{y_i}^{y_i + \delta y} \xi \, dy.$$

The parameter h is effectively a smoothing parameter (the limit $h \to 0$ representing a point vortex) which desingularises the interaction between vortices. Integration of Eq. (11) determines that the stream component of velocity at the point (x_i, y_i) is given by

$$u(x_i, y_i) = U(x_i) + \int_{y_i}^{\infty} \xi \, dy. \tag{13}$$

This equation implies that the stream component of velocity of a vortex sheet segment at a point (x_i, y_i), induced by the surrounding vorticity of the flow, is influenced only by the vorticity distribution above it, i.e., by vortex elements located at vertical positions $\{y_j\}$ such that $y_j > y_i$. In discrete form (13) can be expressed by the approximation

$$u(x_i, y_i) \approx U(x_i) + \tfrac{1}{2}\gamma_i + \Sigma \gamma_j d_j, \tag{14}$$

where $d_j = 1 - |x_i - x_j|/h$ expresses the proportionate horizontal overlap between sheet elements located at (x_i, y_i) and (x_j, y_j). If the downward projection of the jth sheet does not overlap with the sheet at (x_i, y_i), then, to a good approximation, it does not contribute to the induced velocity of the ith sheet. The summation in (14) can be restricted because of this, to overlapping sheets.

The vertical component of velocity at (x_i, y_i) is obtained from the continuity condition (1c) as

$$v(x_i, y_i) = -\frac{\partial}{\partial x} \int_0^{y_i} u \, dy \tag{15}$$

which can be determined also in discrete form by substitution of (14) into the discretised integral of (15). This is expressed by the algorithm (see [1, 15, 16] for derivation details)

$$V_i = -(I^+ + I^-)/h$$

where $$I^{\pm} = U\left(x \pm \frac{h}{2}\right) y_i + \Sigma y_j^0 \gamma_j d_j^{\pm}$$

and $$d_j^{\pm} = 1 - \left| x_i \pm \frac{h}{2} - x_j \right| \Big/ h$$

$$y_j^0 = \min(y_i, y_j).$$

Note in the context of the present application,

$$U\left(x \pm \frac{h}{2}\right) = U_0\left(x \pm \frac{h}{2}\right)^m.$$

Having determined the velocity induced at the ith sheet element, this element is displaced in this field over a time step dt, by $(dx_i, dy_i) = (u, v)\, dt$.

The effects of viscosity are introduced during the second fractional time step; by imparting to each sheet element an independent Gaussian random walk displacement in the y-direction, these displacements having zero mean and standard deviation $\sigma = (2\nu\, dt)^{1/2}$.

At each time-step the boundary conditions must be imposed. The no-slip condition $u(x, 0) = 0$ is re-established by the creation of a vortex sheet at the boundary. If, upon completion of the first fractional time step, $u(x, 0) = u_0 \neq 0$, then a vortex sheet is created at the boundary of intensity $2u_0$ per unit length.

During the second fractional step these newly created sheets are segmented along the boundary. Each such segment is then represented by a number of discrete sheet elements (of length h) which have in summation an intensity $2u_0$, but which individually satisfy a condition $\gamma_i \leqslant \gamma_{\max}$. These elements are made to undergo a random walk in the $\pm y$ direction. In order to describe this diffusion process as one which is isotropic, the boundary layer is formally extended into the region $y < 0$ (see [1]). During the vortex sheet creation process half the newly created vortex sheet elements will on average diffuse into $y > 0$ and half into $y < 0$. This effectively imposes the no-slip condition. Vortex elements which are displaced into the region $y < 0$ immediately after they are created are deleted from the calculation. Vortex elements which are subsequently displaced from the flow into the region $y < 0$, are reflected back into the flow. (An alternative vorticity creation algorithm has been described in Refs. [3, 18].)

The convergence properties of random vortex methods have been investigated by a number of authors [3, 18, 20, 21]. In particular, Puckett [3] demonstrates a favourable dependence of the random sheet method on viscosity for the Blasius case and shows that this same dependence extends to Falkner–Skan flow. This is to say, the method does not become less convergent as $\nu \to 0$. For the Blasius case, the relationship between the rate of convergence and the parameterization was explored numerically by Puckett. Error estimates were evaluated (for the flow at a particular instant of time) and compared for systematic permutations of parameters $\gamma_{\max}$, h, dt. Stream velocity was ensemble-averaged over statistically independent trials of the random walk simulation, and the error estimate (determined from comparison with the Blasius similar solution) was expressed as a discrete L^1 norm. Puckett demonstrates that error decreases as parameters h, dt, and $\gamma_{\max}$ are refined, provided $dt \leqslant h$, and $h = 0\ (\gamma_{\max}^{3/4})$.

There are two important contributions to the numerical stability of the solution procedure. The leading edge, $x = 0$, is a singular point. Real flow at much a leading edge has, of necessity, a significant vertical component and this violates the Prandtl

boundary layer approximation. For cases $m > 0$ the singularity may be sufficiently weak [22, 23] to allow us to neglect its influence on the downstream evolution of the boundary layer. For the case $m < 0$ the external flow is in itself singular at $x = 0$, and this may affect the stability of the downstream solution.

Similarly, the abrupt extinguishing of vorticity at a point downstream may introduce reverse flow and separation which can propagate upstream [1, 5]. The development of this effect could manifest itself during evolution over a long time interval.

The leading edge singularity for $m > 0$ can probably be mitigated by treating the neighbourhood of the edge specially using vortex core elements rather than sheet elements, hence solving there the Navier–Stokes equation rather than Eq. (2). Another approach to this problem is that of treating the upstream and downstream conditions as if they were periodic, invoking similarity scaling to transfer vortex sheets as they leave the solution domain downstream, to re-enter at a point upstream [3].

Since one purpose of the present investigation is to compare similar and non-similar solutions, it does not seem appropriate to impose the property of similarity in the non-similar solution procedure. Certainly this would complicate any comparison which could be made between the two solutions. In order to address the problem of disposing of vortex sheets downstream, the sheets are maintained in the flow after they have left the solution domain along a path extrapolated from their motion at the downstream edge of the boundary [24]. In this way the structure of the boundary layer is approximated in a region beyond the downstream edge of the boundary. No attempt in the present work is made to try to remove the possible effects of the leading edge singularity.

4. Comparison of Velocity Profiles

To demonstrate the method, we consider the case of stagnation flow, that is to say, we consider a boundary layer subject to an external flow given by (4) with $m = 1$. Equation (12) can be made dimensionless by introducing the streamwise Reynolds number $\mathrm{Re}_x = U_0 L/\nu$, where L is a representative scale length in the stream direction. Equation (12) can be written

$$\frac{\partial \xi}{\partial t'} + u' \frac{\partial \xi}{\partial x'} + v' \frac{\partial \xi}{\partial y'} = \frac{1}{\mathrm{Re}_x} \frac{\partial^2 \xi}{\partial y'^2}$$

with $x' = x/L$, $y' = y/L$, and $t' = tU_0/L$. We concentrate our attention on the range $x' \in [0, 1.5]$. We consider a Reynolds number of 10^6, and a time-step increment of $dt' = 0.2$. We restrict the maximum strength of vortex sheet to $\gamma = 0.1$, $h = 0.2$ to conform to the parameters associated with Fig. 2 of [1]. If greater vorticity is required to be created at the boundary to effect the no-slip condition during a time step, then this must be composed of a number of vortex sheet elements, each of strength less than or equal to 0.1.

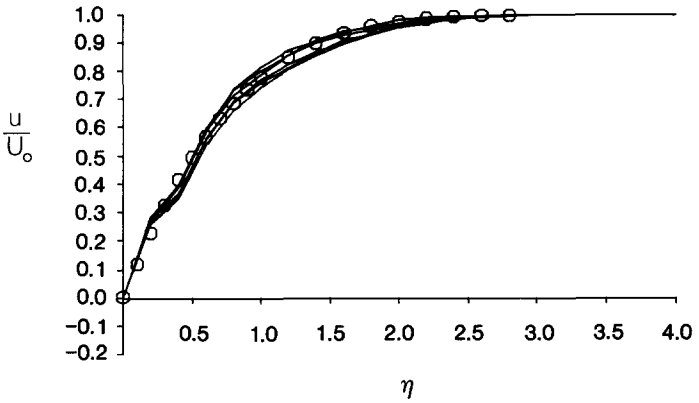

FIG. 1. Stream component of velocity as a function of similarity variable η, for $m = 1$ (stagnation flow case). Each profile (solid lines) corresponds to a 60-step time-average ($dt = 0.2$). The circles indicate the Falkner–Skan solution for $m = 1$.

The stream velocity component is computed at the position $x' = 1$, and this profile is plotted as a function of the similarity variable (6). As time progresses, the velocity profile is averaged in 60-step samples. The successive mean profiles achieved in this way are plotted in Fig. 1. The circles in Fig. 1 represent the stationary Falkner–Skan solution for $m = 1$ (from [8]).

The first such profile will contain the impulsive starting conditions which, by the time the second profile is evaluated, have begun to wash out of the solution. The velocity field appears to converge quite uniformly to the Falkner–Skan profile.

Figure 2 illustrates the velocity profile generated by the random vortex procedure for the Blasius case, $m = 0$. The convergence towards the stationary solution is less rapid and less uniform than was the case for $m = 1$. This to say, the variance from the mean appears to be greater than in the corresponding profiles of Fig. 1.

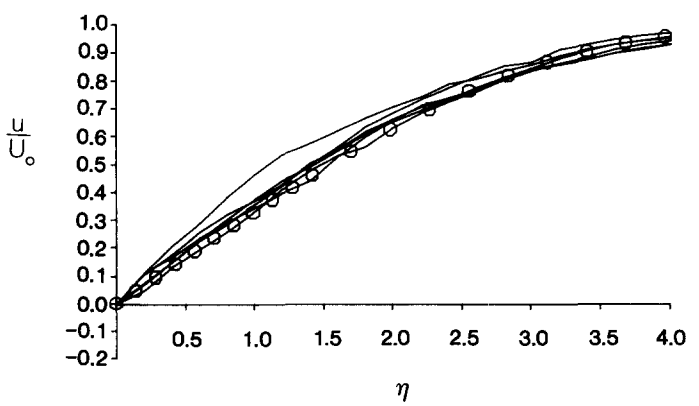

FIG. 2. Same as Fig. 1 for the case $m = 0$ (Blasius flow case).

The situation can be examined in more detail by considering a longer average of the two random vortex solutions illustarted in Figs. 1 and 2. In order to exclude the initial impulsive conditions, we can take a mean from the 120th step to the 360th step, evaluating in both cases the variance from the mean as a function of η. Figures 3 and 4 display a 240-step mean of the stream component and the vertical component for the cases $m=1$ and $m=0$, respectively. The open circles represent the respective Falkner–Skan solutions (from [8]).

The rms dispersion from the mean, or fluctuation intensity, is expressed as a function of η for both u and v in a manner analogous to the evaluation of turbulence intensity. In the stagnation case shown in Fig. 3 this dispersion in $\langle u \rangle$ reaches a maximum at $\eta=0.5$, this maximum being some 20% of the stream velocity there. The dispersion falls sharply as η increases beyond $\eta=0.5$.

On the other hand, the rms dispersion from the mean in the vertical component exceeds the magnitude of $\langle v \rangle$ in $\eta<1$. This is perhaps to be expected, since $\langle v \rangle$ is two or three orders of magnitude less than $\langle u \rangle$ and would conceivably be highly transient near the boundary.

The situation for the Blasius case $m=0$ is illustrated in Fig. 4, where we note the relative broadening of the dispersion curve, the maximum reaching some 50% of the stream velocity in the neighbourhood of $\eta=1$, although this falls to 7% for

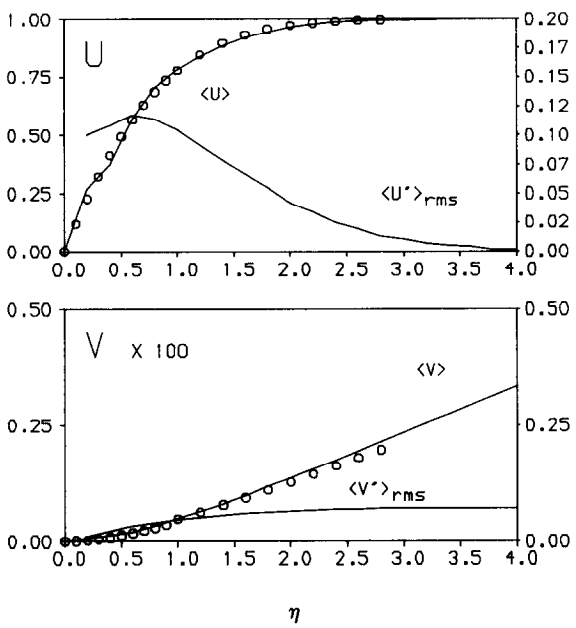

FIG. 3. Horizontal and vertical flow profiles ($\langle U \rangle$, $\langle V \rangle$) averaged over 240 time steps ($dt=0.2$). The open circles indicate the Falkner–Skan equation. The root-mean-squared fluctuation from the means for the random vortex method calculation is also plotted as a function of similarity variable η. The case $m=1$.

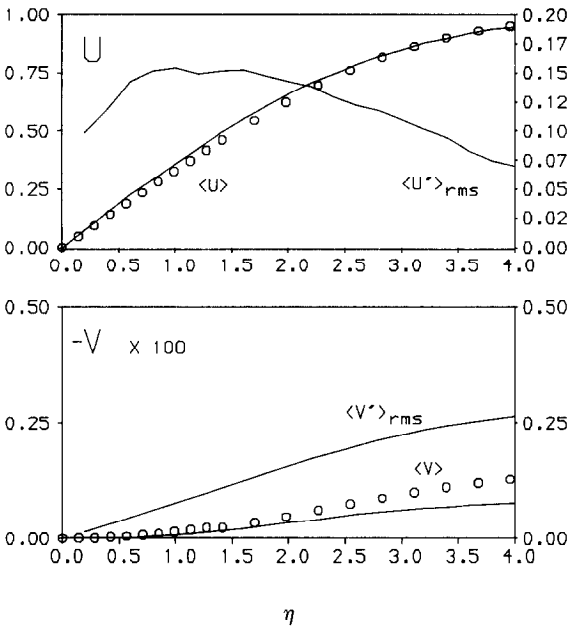

FIG. 4. Same as Fig. 3 for the case $m = 0$.

$\eta = 4$. In the vertical component we note that the magnitude of the dispersion curv $\langle v' \rangle_{\text{rms}}$ exceeds the mean $\langle v \rangle$.

As m decreases from 1 to 0, the fluctuation from the mean during the solutio procedure increases both in magnitude and in its spread in the boundary layer. A indication of this can be seen from a comparison of Figs. 3 and 4. The mean valu of the vertical component is notably smaller in the case $m = 0$ than in the cas $m = 1$, and the fluctuation from the mean is larger in the case $m = 0$ than in the cas $m = 1$.

5. Comparison of Gross Flow Parameters

The stream velocity profile can be integrated to provide two gross flo parameters which characterise a boundary layer. This displacement thickness given by

$$\delta(x) = \int_0^\infty (U(x) - u(x, y))\, dy$$

and the drag (or momentum defect) is given by

$$\theta(x) = \int_0^\infty u(x, y)(U(x) - u(x, y))\, dy.$$

Both drag and displacement thickness can be formulated in a computationally efficient way in terms of the random vortex model (see [1]). If δ and θ are to be evaluated at a position X, we can consider those sheet elements in a slice of the boundary such that $|x_i - X| < h$. If there are M such elements in the slice, and if they are sorted and labelled so that $y_1 \leqslant y_2 \leqslant \cdots \leqslant y_M$, then we can write

$$\delta \approx \sum_{i=1}^{M} (U(x_i) - u_i)\, \Delta y_i,$$

where u_i is given by (14) and $\Delta y \equiv y_i - y_{i-1}$. In this way the vertical distance between successive sheets is exploited as an interval of integration. The drag can similarly be approximated by

$$\theta \approx \sum_{i=1}^{M} u_i (U(x_i) - u_i)\, \Delta y_i.$$

The gross flow parameters determined in this way from the random vortex simulation can be compared to those calculated from the Falkner–Skan solutions the latter have been tabulated in Table 4-2 in [25], for example.

In Fig. 5 the displacement thickness, δ, is evaluated as a succession of averages taken over 60 time steps, and sampled at ten 60-step intervals during a 600-step computation. These time averages of δ are indicated by the open circles for the

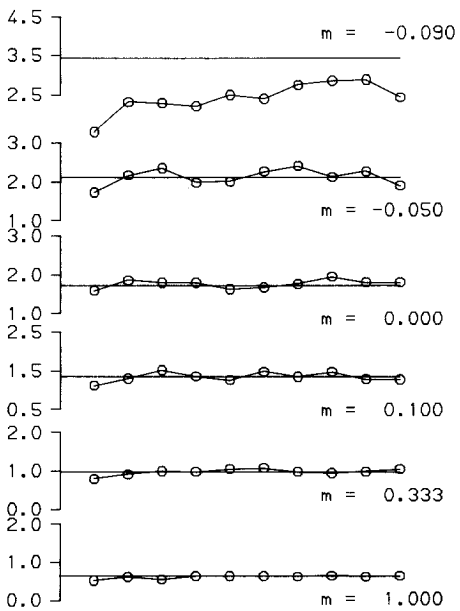

FIG. 5. Displacement thickness for various values of m evaluated during a 600 time-step computation.

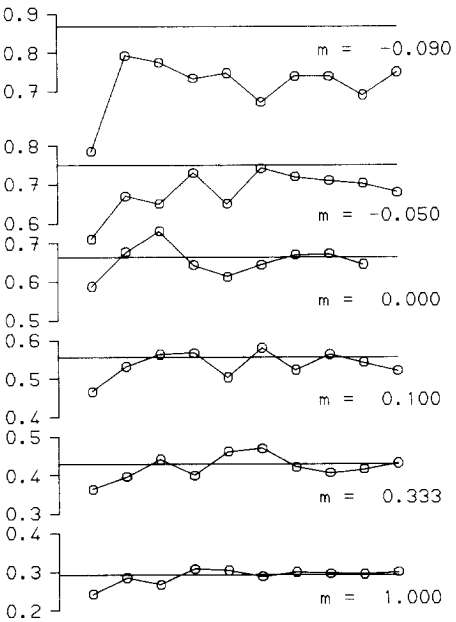

FIG. 6. Drag for various values of m during a 600 time-step computation. Each estimate (open circles) consists of a 60-step mean. The horizontal line represents the Falkner–Skan evaluation of drag.

TABLE I

Comparison of Time-Averaged Displacement Thickness with the Solution to the Falkner–Skan Equation

	$\frac{\delta}{x}\sqrt{\text{Re}}$		
m	RVM	SD	F–S
1	0.631	0.04	0.648
1/3	0.984	0.08	0.985
0.1	1.32	0.1	1.348
0.0	1.707	0.1	1.721
−0.05	2.12	0.2	2.117
−0.0904	2.42	0.4	3.428

Note. Average taken over 600 time steps, $dt = 0.1$. SD is the standard deviation.

TABLE II

Comparison of Time-Averaged Drag with the Similar Solution to the Falkner–Skan Equation

	$\frac{\theta}{x}\sqrt{\mathrm{Re}}$		
m	RVM	SD	F–S
1	0.297	0.02	0.292
1/3	0.421	0.03	0.429
0.1	0.528	0.04	0.557
0.0	0.659	0.04	0.664
−0.05	0.682	0.05	0.751
−0.0904	0.719	0.07	0.868

indicated values of $m \in [-0.0904, 1]$. The horizontal lines represent the corresponding values derived from similar solutions. Fig. 6 illustrates the comparison for drag.

These comparisons (see Tables I and II) demonstrate that the agreement between similar and random vortex solutions becomes less close as the parameter m becomes negative. The random vortex method evaluation of drag and displacement thickness departs most strongly from the similar solution at $m = -0.0904$. However, since $m = -0.0904$ represents the exponent at which flow becomes separated, it is difficult to interpret these particular gross flow parameters, which are, after all, intended to characterise an attached boundary layer.

6. Visualisation of Boundary Layer Flow Structure

The random vortex method provides a grid-free solution procedure which can, in principle, determine the development in time of a laminar boundary layer. For example, if we examine the evolving flow solutions within a regime $6 \times \mathrm{Re}_x^{-1/2}$ of the boundary $y = 0$, we find at $m = 1$ a relatively stable stagnation flow develops within

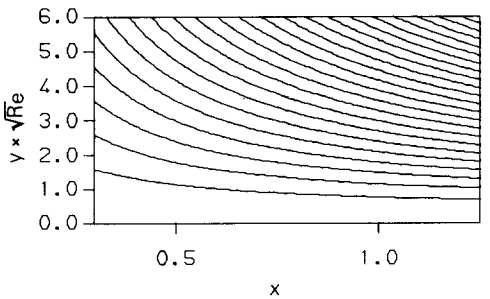

FIG. 7. Stream lines of flow for averaged flow in the case $m = 1$ (stagnation).

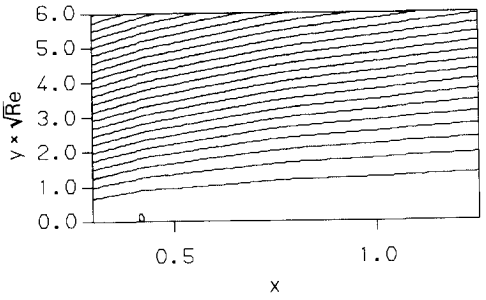

FIG. 8. Same as Fig. 7 for the case $m = -0.05$.

100 time steps of start up ($t = 0$, $dt = 0.2$). As m becomes smaller on $m \in (1, 0)$ the flow is characterised by oscillations of increasing amplitude. On $m \in (0, -0.0904)$ reverse flow modes develop. A statistically sensible visualisation of the boundary layer flow structure requires that a time average be taken over these oscillatory and reverse flow modes.

Figure 7 illustrates a 100-step average ($dt = 0.2$) of the flow associated with $m = 1$. The diagram is a map of the stream lines in the regime $0.25 \leqslant x \leqslant 1.5$ and $0 \leqslant y \leqslant 6\,\mathrm{Re}_x^{-1/2}$. The character of stagnation flow has obviously evolved. Note that the vertical scale on this diagram is some $\mathrm{Re}^{1/2}$ greater than the horizontal scale and this serves to exaggerate the vertical motion for purposes of graphical visualisation.

Figure 8 illustrates the stream lines associated with the case $m = 0.05$. The vertical motions associated with the instantaneous oscillatory modes tend upon time averaging to zero. Therefore, the mean flow still appears that of an attached boundary layer.

Figure 9 illustrates the stream lines associated with the case $m = -0.2$. Since this is in the parameter range $m < -0.0904$, from boundary layer theory we would expect this to be a case of separated flow. Indeed, the stream lines derived from the random vortex method illustrate just such a fully separated flow with a bubble of reverse flow along the boundary.

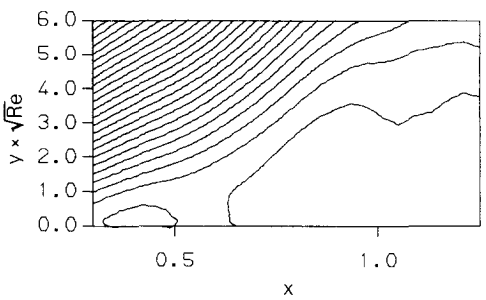

FIG. 9. Same as Fig. 7 for the case $m = -0.20$ (separation).

7. Conclusions

The random vortex method is applied with considerable success to the problem of Prandtl boundary layer flow subject to an external velocity of the form $U(x) = U_0 x^m$, the stationary solution to this problem being that of Falkner–Skan flow. The time-averaged stream velocity profiles compare well with the similar solutions to the Falkner–Skan equation. The variance from the mean was also calculated for the random vortex method mean flows. The dependence of this "fluctuation intensity" on similarity variable, η, resembles qualitatively the structure of streamwise and vertical turbulence intensities on η (see Fig. 7-17 of Ref. [22]). The variances associated with the mean values $\langle u \rangle$ and $\langle v \rangle$ increase as m decreases on the range $m \in [0, 1]$. In fact, the agreement between the Falkner–Skan solution for v and the mean $\langle v \rangle$ becomes less close as m decreases, although the similar solution curve lies well within the standard deviation of $\langle v \rangle$.

The gross flow parameters of drag, θ, and displacement thickness, δ, averaged over successive 60-step intervals during a 600-step computation have been compared for $m = \{-0.0904, -0.05, 0, 0.1, 0.333, 1.0\}$ with the parameters derived from the Falkner–Skan solutions. These random vortex sheet averages show good agreement to the similar solution; again, as m becomes negative, the agreement with similar solutions begins to deteriorate. At $m = -0.0904$ (the point, according to analysis of similar solutions, at which the skin friction should vanish and separation ensue) the gross flow parameters determined from the random vortex method are considerably less than that expected from the similar solution.

Because the random vortex method is grid-free, it can, in principle, provide a flow visualisation of the dynamics in the immediate neighbourhood of the boundary. Although for $m > 0$, oscillatory structures are convected downstream, upon time-averaging the vertical velocities associated with them, tend to a relatively small mean. For $m < 0$, the development of separation can be observed in the streamline depiction of the random vortex solution: the oscillatory structures appear to become recirculating structures in this regime.

The Falkner–Skan similar solution is consistent with a pressure field which derives its structure from the external flow. On the other hand, non-similar solutions to the vorticity representation of the boundary layer equations, as well as being non-stationary, are also unconstrained in their pressure field. The question of convergence should be understood in the context of a flow with impulsive starting conditions, followed by an interval of transience as the boundary layer evolves into a presumed steady state. The character of the fully developed flow will depend upon whether the time-dependent solution to equation (12) tends asymptotically to a flow which is strictly time steady in the limit $t \to \infty$, or whether the vorticity dynamics of a developed boundary layer retains any essential time dependence.

If the fully developed boundary layer is strictly time steady, then the random vortex sheet solution for this flow should exhibit time fluctuations associated entirely with the stochastic model of diffusion. An examination of the instantaneous

velocity field (u, v) resulting from the present vortex sheet simulation suggests a more complex vortical evolving flow, which nevertheless has a stationary mean.

The notion that self-similar solutions to (2) correspond to steady states of a time-dependent process is an interesting conjecture [13]. In the parameter range $m \in [-0.05, 1]$ the numerical evidence of the present work supports this conjecture: the random vortex sheet solution for time-dependent boundary layer flow does give, in time average, a flow which approximates well the Falkner–Skan flow solutions. The existence of solutions to the Falkner–Skan equation which are periodic in space or which consist of reverse flow modes does seem to be consistent with the evolving flow whose dynamics, in time average, are depicted in Figs. 7–9.

The stability of these time-dependent solutions may also be related to initial conditions and to conditions in the neighbourhood of the singular point $x = 0$. It is interesting to note that Serrin [23] has shown, in the context of the steady flow problem, that similar solutions asymptotically develop downstream, irrespective of conditions at $x = 0$. The implications of leading edge conditions to the vortex sheet solution of the time-dependent equations (12) for Falkner–Skan flow remains to be investigated.

Acknowledgment

The author thanks Professor A. J. Chorin for his interest in this work.

References

1. A. J. Chorin, *J. Comput. Phys.* **27**, 428 (1978).
2. H. Schlichting, *Boundary-Layer Theory* (McGraw–Hill, New York, 1968), p. 117.
3. E. G. Puckett, *SIAM J. Sci. Statist. Comput.* **10**, 298 (1989).
4. R. I. Lewis, in *Seventh Conference on Fluid Machinery, Budapest, Hungary, 1983.*
5. R. I. Lewis and D. T. C. Porthouse, University of Newcastle-upon-Tyne Report No. Tb 60, 1983 (unpublished).
6. W. A. Coppel, *Philos. Trans. Roy. Soc. London A* **253**, 101 (1960).
7. A. H. Craven and L. A. Peletier, *Mathematika* **19**, 129 (1972).
8. D. R. Hartree, *Proc. Cambridge Philos. Soc.* **33**, 223 (1937).
9. T. Cebeci and H. B. Keller, *J. Comput. Phys.* **7**, 289 (1971).
10. P. A. Libby and T. M. Liu, *AIAA J.* **5**, 1040 (1967).
11. K. Stewartson, *Proc. Cambridge Philos. Soc.* **50**, 454 (1953).
12. S. P. Hastings, *SIAM J. Appl. Math.* **22**, 329 (1972).
13. S. P. Hastings and W. Troy, *Proc. Roy. Soc. London A* **397**, 415 (1985).
14. E. F. F. Botta, F. J. Hut, and A. E. P. Veldman, *J. Eng. Math.* **20**, 81 (1986).
15. A. J. Chorin, *SIAM J. Sci. Statist. Comput.* **1**, 1 (1980).
16. A. Y. L. Cheer, *SIAM J. Sci. Statist. Comput.* **4**, 685 (1983).
17. A. F. Ghoniem, A. J. Chorin, and A. K. Oppenheim, *Philos. Trans. Roy. Soc. London A* **304**, 303 (1982).
18. J. A. Sethian and A. F. Ghoniem, *J. Comput. Phys.* **74**, 283 (1988).

19. A. Y. CHEER, Lawrence Berkeley Laboratory Report LBL-6443 Suppl., Berkeley, California, 1978 (unpublished).
20. G. BENFATTO AND M. PULVIRENTI, *Commun. Math. Phys.* **96**, 59 (1984).
21. O. HALD, *SIAM J. Sci. Statist. Comput.* **7**, 1373 (1986).
22. K. STEWARTSON, *The Theory of Laminar Boundary Layers in Compressible Fluids* (Oxford Univ. Press, Oxford, 1964), p. 66.
23. J. SERRIN, *Proc. Roy. Soc. London A* **299**, 491 (1967).
24. A. J. CHORIN, Department of Mathematics, University of California, Berkeley, private communication (1987).
25. J. A. SCHETZ, *Foundations of Boundary Layer Theory* (Prentice–Hall, New York, 1984), p. 71.